Linear semi-infinite programming approach for entanglement quantification

Thiago Mureebe Carrijo,* Wesley Bueno Cardoso, and Ardiley Torres Avelar
Instituto de Física, Universidade Federal de Goiás, 74.690-900, Goiânia, Goiás, Brazil

(Received 29 July 2020; accepted 20 July 2021; published 16 August 2021)

We explore the dual problem of the convex roof construction by identifying it as a linear semi-infinite programming (LSIP) problem. Using the LSIP theory, we show the absence of a duality gap between primal and dual problems, even if the entanglement quantifier is not continuous, and prove that the set of optimal solutions is nonempty and bounded. In addition, we implement a central cutting-plane algorithm for LSIP to quantify entanglement between three qubits. The algorithm has global convergence property and gives lower bounds on the entanglement measure for nonoptimal feasible points. As an application, we use the algorithm for calculating the convex roof of the three-tangle and π-tangle measures for families of states with low and high ranks. Since the π-tangle measure quantifies the entanglement of W states, we apply the values of the two quantifiers to distinguish between the two different types of genuine three-qubit entanglement.

DOI: 10.1103/PhysRevA.104.022413

I. INTRODUCTION

Quantum entanglement is a special type of correlation of quantum systems with two or more parts, which admit global states that cannot be written as a product of the states of the parts. The interest in this phenomenon has origin in its importance in fundamental questions of quantum mechanics, including the Einstein-Podolski-Rosen paradox [1] and nonlocality [2,3], in its relationship with other physical phenomena such as super-radiance [4,5] and superconductivity [6,7], and in technological applications in the fields of quantum computing, quantum information [8,9], and quantum metrology [10]. As a consequence, the production, manipulation, and quantification of entanglement are permanent topics of scientific interest. In particular, the quantification of entanglement can be accomplished using several different types of entanglement measures that are generally much simpler to define for pure states than for mixed states. Fortunately, the construction of a measure for mixed states can be done through the convex roof of an entanglement monotone [11]. However, the calculation of a convex roof is computationally expensive for high-rank states, except for a few cases whose analytical solution is known [12,13].

Most numerical algorithms for the convex roof calculations work to find the optimal pure state decomposition of the input state [14–18]. Although this approach can be very efficient for low-rank states, the parameter space of the optimization problem grows quickly with rank and has a maximal number of parameters of $\sim 2n^3$ [19], where n is the dimension of the system. Also, these methods usually lack global convergence, which means that they can guarantee only upper bounds on the optimal value. Another method obtains a sequence of lower bounds by solving semidefinite programming problems, but only for measures that are polynomials of expectation values of observables for pure states [20]. A promising approach, with fewer optimization parameters, consists of solving the dual problem of the convex roof optimization task [21]. Following this idea, a minimax algorithm that provides a verifiable globally optimal solution or a lower bound on the convex roof measure was proposed for the dual problem [19].

The concept of genuine multipartite entanglement, which applies to systems with three or more parts, is a type of entanglement that cannot be described as a correlation in a bipartite partition only [8,22]. It is present in many quantum algorithms [23,24], cryptographic protocols [25–27], and quantum phenomena [28–30]. As a resource, it is essential to be able to quantify it by quantifiers like the three-tangle [31], the generalization of the three-tangle by means of hyperdeterminants [32], the π-tangle [33], and others [34]. Analytical formulas for these measures are known only for special families of states, which means that a numerical approach is usually required.

Here, we explore the dual problem of the convex roof optimization procedure and show that it is a linear semi-infinite programming (LSIP). We also prove some properties of the optimization problem using the LSIP theory and describe the characteristics of a central cutting-plane algorithm (CCPA) adapted to solve the dual problem. In addition, to show how this method performs in practice, we implement the algorithm in the MATLAB language and calculate the multipartite entanglement quantifiers for two families of three-qubit states. The selected measures are the three-tangle and the π-tangle, both entanglement monotones that quantify genuine tripartite entanglement. We choose a mixture of Greenberger-Horne-Zeilinger (GHZ) and W states as one of the families, and the generalized Werner states, a class of states with full rank, as the other one. Finally, we numerically calculate the quantifiers and compare them with analytical values available in the literature.

II. BASIC CONCEPTS

A. Three-tangle

Concurrence is an entanglement measure for the state ρ of two qubits defined as $\mathcal{C}(\rho) \equiv \max\{0, \lambda_1 - \lambda_2 - \lambda_3 - \lambda_4\}$,

*thiagomureebe@gmail.com

where $\lambda_1, \ldots, \lambda_4$ are the eigenvalues of the matrix $\sqrt{\sqrt{\rho}\tilde{\rho}\sqrt{\rho}}$ in decreasing order and $\tilde{\rho} \equiv (\sigma_y \otimes \sigma_y)\rho^*(\sigma_y \otimes \sigma_y)$, with σ_y as a Pauli spin matrix [35]. To make the notation more economical, we symbolize a pure state of set of density matrices Ω as $[\psi] \equiv |\psi\rangle\langle\psi|$, where $|\psi\rangle$ is a normalized vector of the Hilbert space $\mathcal{H}$ of the system. Then, for a state $|\psi\rangle$ of three qubits with partition $A(BC)$, the concurrence is defined as $\mathcal{C}_{A(BC)}([\psi]) \equiv \sqrt{2[1 - \mathrm{Tr}(\rho_A^2)]}$, where $\rho_A \equiv \mathrm{Tr}_{BC}([\psi])$. For pure states, the three-tangle τ is then defined as $\tau([\psi]) = \mathcal{C}^2_{A(BC)}([\psi]) - \mathcal{C}^2(\rho_{AB}) - \mathcal{C}^2(\rho_{AC})$, where $\rho_{AB} \equiv \mathrm{Tr}_C([\psi])$ and $\rho_{AC} \equiv \mathrm{Tr}_B([\psi])$ [31]. It is a measure of genuine three-qubit entanglement and it is defined, for mixed states, as the convex roof in relation to the set of pure states $\mathcal{E}$:

$$\tau(\rho) \equiv \inf_{\{p_k, |\psi_k\rangle\}} \sum_k p_k \tau([\psi_k]), \tag{1}$$

such that $\sum_k p_k[\psi_k] = \rho$, where $\sum_k p_k = 1$, $p_k \geqslant 0$, $[\psi_k] \in \mathcal{E}$, and the infimum is taken over all possible pure state decompositions of ρ.

The three-tangle has analytical expressions for some families of states. For example, the families $\rho_p \equiv p[\mathrm{GHZ}] + (1 - p)[\mathrm{W}]$ [12,13] and $\rho'_p \equiv p[\mathrm{GHZ}] + (1 - p)\mathbb{1}/8$ [36], where $|\mathrm{GHZ}\rangle \equiv (|000\rangle + |111\rangle)/\sqrt{2}$ and $|W\rangle \equiv (|001\rangle + |010\rangle + |100\rangle)/\sqrt{3}$ (namely GHZ and W states, respectively). Formulas are available in Appendix B.

For future reference, we introduce the definitions of three classes of three-qubit mixed states: B, W, and GHZ [37]. The class B of biseparable states is the set of density matrices that can be expressed as a convex sum of tensor products of qubit states with two-qubit states. To define the W class, we need the concept of W-type states, which are those that can be written as $\lambda_0|000\rangle + \lambda_1|100\rangle + \lambda_2|101\rangle + \lambda_3|110\rangle$, where $\lambda_0 \geqslant 0$ and $\lambda_k > 0$ for $k > 0$ [38]. So, the class W is the set of states that are a convex sum of W-type states or biseparable states. Finally, the class GHZ is the set of all mixed three-qubit states.

B. π-tangle

An important quantifier of genuine three-qubit entanglement for pure states is called π-tangle, or three-π [33]. It is based on negativity [39], an entanglement monotone given by $\mathcal{N}_{AB}(\rho) \equiv \|\rho^{T_A}\|_1 - 1$, where $\|.\|_1$ is the trace norm, ρ^{T_A} is the partial transpose of ρ in relation to the subsystem A, and the multiplicative constant "1/2" has been removed. Let $[\psi] \in \mathcal{E}$ be a state of a three-qubit system ABC and $\pi_A([\psi]) \equiv \mathcal{N}^2_{A(BC)}([\psi]) - \mathcal{N}^2_{AB}(\rho_{AB}) - \mathcal{N}^2_{AC}(\rho_{AC})$, where $\mathcal{N}_{A(BC)}([\psi]) = \|[\psi]^{T_A}\|_1 - 1$. Functions π_B and π_C are defined analogously. The π-tangle quantifier is then defined as $\pi([\psi]) \equiv [\pi_A([\psi]) + \pi_B([\psi]) + \pi_C([\psi])]/3$.

As proved in Ref. [33], the π-tangle is an entanglement monotone and vanishes for product state vectors, qualifying it as a measure of entanglement [40]. Also, it is an upper bound on the three-tangle: $\pi([\psi]) \geqslant \tau([\psi])$, implying that it is strictly positive for the states of the GHZ\W class [38], which is the GHZ class with the exception of the states of the W class [37]. Moreover, it is also strictly positive for states of the W class with the form $|\psi\rangle = \alpha|100\rangle + \beta|010\rangle + \gamma|001\rangle$ and, according to numerical calculations [33], this is valid for other pure states of the W\B class, which is the W class with the exception of the states of the B class. For mixed states, the convex roof of the π-tangle was calculated only for the mixture ρ_p of W and GHZ states [41].

C. Convex roof duality

Before talking about the dual problem of the convex roof procedure, let us introduce some notation and definitions. Let $\mathbb{R}^{(\mathcal{E})}$ be the set of all functions $f : \mathcal{E} \to \mathbb{R}$ that have finite support. This is a kind of "generalized sequence" space, with only finite "sequences" of real numbers indexed by the set $\mathcal{E}$. Also, the set $\mathbb{R}^{(\mathcal{E})}$ is a vector subspace of the space of real functions with $\mathcal{E}$ as domain. Defining E as a non-negative continuous entanglement monotone for pure states, its convex roof $E^{\cup}$ is given by the optimization problem P:

$$\begin{aligned} &\min_{f \in \mathbb{R}^{(\mathcal{E})}} && \sum_{[\psi] \in \mathcal{E}} f([\psi])E([\psi]), \\ &\text{subject to} && \sum_{[\psi] \in \mathcal{E}} f([\psi])[\psi] = \rho, \quad f \geqslant 0. \end{aligned} \tag{2}$$

Equation (2) means that the optimization goal of problem P, called the primal problem, is to minimize the first sum, satisfying the conditions imposed by the equality and the inequality presented. Associated with P, there is the dual problem, which provides a lower bound to the optimal value of P. A dual problem can be obtained in several ways from the primal one, but the most typical is obtained through the construction of the Lagrangian of P and its subsequent minimization, resulting in the dual D [21,42]:

$$\begin{aligned} &\sup_{X \in H} && -\mathrm{Tr}(\rho X), \\ &\text{subject to} && E([\psi]) + \mathrm{Tr}([\psi]X) \geqslant 0, \ \forall [\psi] \in \mathcal{E}, \end{aligned} \tag{3}$$

with H as the space of n-dimensional Hermitian matrices. As D has linear objective function, a finite number of variables (setting a base in H, we have n^2 real variables) and an infinite number of linear inequalities, the problem is a LSIP [43].

III. THE LSIP APPROACH

A. Properties of P and D

We are going to reformulate the problem D according to the eigendecomposition of $\rho = \sum_{k=1}^r \lambda_k[\phi_k]$, where r is the rank of ρ. If $|\phi_1\rangle, \ldots, |\phi_r\rangle$ are orthonormal eigenvectors of ρ, then any other pure state decomposition $\rho = \sum_l p_l[\psi_l]$ satisfies $|\psi_l\rangle \in \mathcal{H}_\rho \equiv \mathrm{span}\{|\phi_1\rangle, \ldots, |\phi_r\rangle\}, \forall l$, where $\mathrm{span}(S)$ is the linear span of the set S. Defining $\mathcal{E}_\rho \equiv \{[\psi] \in \mathcal{E} : |\psi\rangle \in \mathcal{H}_\rho\}$ and H_ρ as the set of Hermitian operators on $\mathcal{H}_\rho$, the reformulation of D is then given by D_ρ:

$$\begin{aligned} &-\inf_{X \in H_\rho} && \mathrm{Tr}(\rho X), \\ &\text{subject to} && E([\psi]) + \mathrm{Tr}([\psi]X) \geqslant 0, \ \forall [\psi] \in \mathcal{E}_\rho. \end{aligned} \tag{4}$$

In Appendix A, we proved some theoretical properties of problems P and D_ρ in order to allow us to solve problem P by solving problem D_ρ using the algorithm described in the next section. These properties are as follows:

(1) There is no duality gap between P and D_ρ, even for a discontinuous E.

(2) There exists an optimal solution X_ρ^* of D_ρ.

(3) The set of all optimal solutions F_ρ^* of D_ρ is bounded.

By "no duality gap," we mean that the optimal values $v(P)$ and $v(D_\rho)$ of problems P and D_ρ, respectively, are equal. So, we can focus on the solution of D_ρ instead of P. To verify if a solution of problem D_ρ is optimal, we can use one of several known optimality conditions, many of which are described by Theorem 7.1 of Ref. [44]. These conditions are applied on X and, if they are satisfied, then $\mathrm{Tr}(\rho X) = v(D_\rho)$. A common one is the Karush-Kuhn-Tucker sufficient condition, described by the relation $\rho \in A(X)$, where $A(X) \equiv \mathrm{cone}(\mathcal{E}_\rho(X)) = \{\sum_{k=1}^{n} \alpha_k[\psi_k] : [\psi_k] \in \mathcal{E}_\rho(X), \alpha_k \geqslant 0, n \in \mathbb{N}\}$ and $\mathcal{E}_\rho(X) \equiv \{[\psi] \in \mathcal{E}_\rho : E([\psi]) + \mathrm{Tr}([\psi]X) = 0\}$. Since $\mathrm{Tr}(\rho) = 1$, this condition can be reformulated as $\rho \in \mathrm{conv}(\mathcal{E}_\rho(X))$, where $\mathrm{conv}(\mathcal{E}_\rho(X))$ is the convex hull of $\mathcal{E}_\rho(X)$, which is the global optimality condition described in Ref. [19,45].

The linear semi-infinite system of D_ρ is defined as a set of inequalities given by $\sigma_\rho \equiv \{E([\psi]) + \mathrm{Tr}([\psi]X) \geqslant 0, \psi \in \mathcal{E}_\rho\}$, where the set of solutions of σ_ρ is the feasible set F_ρ. By Eq. (4), any valid solution of D_ρ must be a feasible point, which is a point that belongs to F_ρ. There is a relationship between feasible and optimal points of D_ρ and the so-called entanglement witnesses [21]. An entanglement witness Y is a Hermitian operator that is not positive semidefinite and satisfies $\mathrm{Tr}(\rho_{\mathrm{sep}} Y) \geqslant 0$ for any separable state ρ_{sep} [46]. For the definition of an optimal witness, we use an arbitrary bounded set $\mathcal{C}$ and define the set $\mathcal{M} \equiv \mathrm{cl}(\mathcal{W} \cap \mathcal{C})$, where $\mathrm{cl}(\mathcal{W} \cap \mathcal{C})$ is the closure of $\mathcal{W} \cap \mathcal{C}$ and $\mathcal{W}$ is the set of all entanglement witnesses. Then, an entanglement witness Y^* is ρ optimal if $\mathrm{Tr}(\rho Y^*) = \min_{Y \in \mathcal{M}} \mathrm{Tr}(\rho Y)$ [21,47]. If $E([\psi]) = 0$ for any separable state $|\psi\rangle$, it can be verified that any optimal solution $X_\rho^* \neq 0$ of problem D_ρ is a ρ-optimal entanglement witness (the set $\mathcal{C}$ can be any bounded set such that $F_\rho^* \subseteq \mathcal{C}$). In addition, any feasible X such that $\mathrm{Tr}(\rho X) < 0$ is an entanglement witness.

B. Central cutting-plane algorithm

To numerically solve a LSIP problem, several methods are available, mostly classified into five categories: discretization methods, local reduction methods, exchange methods, simplex-like methods, and descent methods, ordered in decreasing order of efficiency according to Ref. [44]. Besides these approaches, other deterministic types of algorithms and uncertain LSIP methods are discussed in a recent review of the field [48]. Because of its efficiency, we choose the CCPA [49] to tackle problem D_ρ, which is classified as a discretization method. For the sake of simplicity, we work with the first version of the algorithm, while subsequent improvements are found in Part IV of Ref. [44] and in Ref. [50]. The CCPA has the advantage of having the property of global convergence, unlike the reduction procedure and almost all methods based on the primal problem P, such as the usual algorithms implemented for calculating the convex roof [14–18]. Also, it generates a sequence of feasible points that converges to an optimal value or to a limit point of an optimal value, implying that a convergent sequence of lower bounds is generated.

In order to successfully employ the CCPA, some conditions need to be satisfied by D_ρ. According to Ref. [49], we need to restrict the feasible set F_ρ to the set $F_\rho' \equiv F_\rho \cap \mathcal{C}$, where $\mathcal{C} \subset H_\rho$ is a compact convex set. Since F_ρ^* is bounded, there exists $\delta > 0$ such that $F_\rho^* \subseteq B_\delta$, where $B_\delta \equiv \{X \in H_\rho : \|X\| \leqslant \delta\}$, with $\|.\|$ as the operator norm, is a compact convex set. As a consequence, choosing an orthonormal basis $\{Z_1, \ldots, Z_{r^2}\}$ for H_ρ, we have the following proposition, whose proof is given in Appendix C:

Corollary 1. Let $\{Z_1, \ldots, Z_{r^2}\}$ be an orthonormal basis of H_ρ, $r = \mathrm{rank}(\rho)$ and $\lambda_1 \leqslant \cdots \leqslant \lambda_r$ the eigenvalues of ρ. If $X \in F_\rho^*$, then $x_m' \equiv |\mathrm{Tr}(Z_m X)| \leqslant r(r-1)\lambda_r/\lambda_1$, for all $m \in \{1, \ldots, r^2\}$.

Other nontrivial conditions are the existence of a nonoptimal Slater point X and the continuity of E. A Slater point X is a point that satisfies $E([\psi]) + \mathrm{Tr}([\psi]X) > 0, \forall [\psi] \in \mathcal{E}_\rho$. Any positive definite matrix $X \in H_\rho$ satisfies this condition, since E is non-negative. Also, if X is optimal, there exists $\alpha > 0$ such that αX is nonoptimal. So, there exists a nonoptimal Slater point for problem D_ρ.

To make the optimization problem easier to solve, we use the result of Corollary 1 and replace the problem D_ρ by the problem D_c:

$$\begin{aligned} &-\inf_{x \in \mathbb{R}^{r^2}} \quad \langle c, x\rangle, \\ &\text{subject to} \quad \tilde{E}(\psi) + \langle \psi, x\rangle \geqslant 0, \quad \forall \psi \in \tilde{\mathcal{E}}_c, \\ &\qquad\qquad |x_m| \leqslant r(r-1)\frac{\lambda_r}{\lambda_1}, \quad 1 \leqslant m \leqslant r^2, \end{aligned} \tag{5}$$

where $X = \sum_k x_k Z_k$, $\rho = \sum_k c_k Z_k$, $\psi \equiv (\psi_1, \ldots, \psi_{r^2})$, $x \equiv (x_1, \ldots, x_{r^2})$, $c \equiv (c_1, \ldots, c_{r^2})$, $\tilde{\mathcal{E}}_c \equiv \{\psi \in \mathbb{R}^{r^2} : \sum_k \psi_k Z_k \in \mathcal{E}_\rho\}$, and $\tilde{E}(\psi) \equiv E([\psi])$. To simplify the discussion of the CCPA, we omit the deletion rules in the pseudocode present in Ref. [49], as they are not necessary for the convergence of the algorithm. The pseudocode of the CCPA in Ref. [49], for a tolerance $\epsilon > 0$, can be found described in Appendix D. The algorithm always terminates and, dropping the tolerance requirement, it generates a sequence of feasible points $\{w^{(k)}\}_{k=0}^{\infty}$ that has limit points which are optimal, meaning that the CCPA has global convergence [49].

IV. NUMERICAL CALCULATIONS FOR π-TANGLE AND THREE-TANGLE

We implement the CCPA in MATLAB for numerical calculations and use it to calculate the π-tangle and the three-tangle for two families of states: ρ_p and ρ_p'. We also compare the numerical calculations with the analytical formulas available in the literature and explicitly described in Appendix B. The results for the states ρ_p expressed in Fig. 1 show good agreement with the analytical curves. With a tolerance $\epsilon = 10^{-3}$, we achieve these results in a few minutes using a common notebook. For the states ρ_p', setting $\epsilon = 10^{-5}$, the numerical three-tangle is slightly lower than the exact nonzero values, according to Fig. 2. This agrees with the fact that the CCPA gives a lower bound on the convex roof when it finds a feasible suboptimal solution. As the CCPA has global convergence, one can generate a larger sequence of feasible points that gives values closer to the exact one. For ρ_p', sequences of

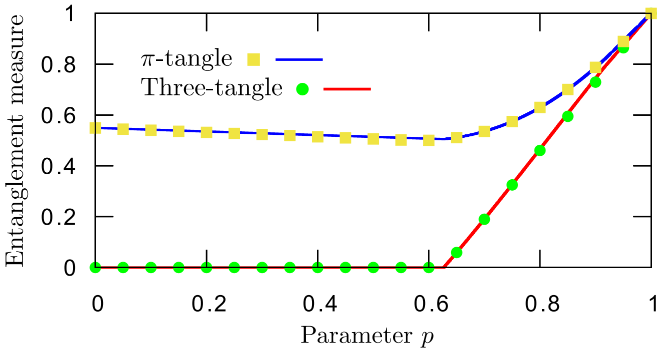

FIG. 1. Three-tangle and π-tangle calculated for states ρ_p. Symbols (boxes and circles) and continuous lines represent numerical and analytical values, respectively.

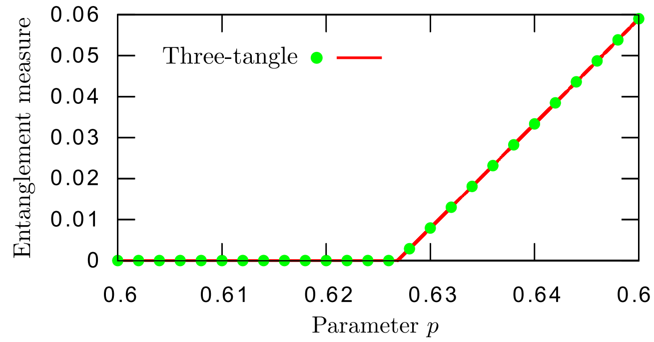

FIG. 3. Three-tangle calculated for states ρ_p. Symbols (circles) and the continuous line represent numerical and analytical values, respectively.

no more than 12 feasible solutions were generated for each value of p and each calculation took a few hours. Since ρ'_p is a rank-8 family of states, this higher computational cost is justified as ρ_p has only rank 2. The calculation time for each state was similar for both measures. So, from the results presented and the analysis of the algorithm, the calculation of convex roof measures, whose restriction for pure states is of similar complexity to those described here and for systems with more dimensions or subsystems, will only consume significantly more time for states of rank greater than 8.

The three-tangle and π-tangle measures can be used to discriminate among the classes B, W\B, and GHZ\W [33]. For the family of states ρ_p, the analytical results in Refs. [12,13], and described in Appendix B, show that ρ_p belongs to the W\B class for $p \lesssim 0.627$ and to the GHZ\W class for higher values of p. As shown by Fig. 1, the positive values of the three-tangle indicate the GHZ\W class, whereas the positive values of the π-tangle in the region where the three-tangle is zero show that the state belongs to the W\B class. The graph around the class transition point, calculated with a tolerance $\epsilon = 10^{-5}$ and depicted in Fig. 3, shows a good agreement between the analytical and numerical results. In the case of the family ρ'_p, it belongs to the B class for $p \leqslant p_B \equiv 3/7 \approx 0.429$, to the W\B class for $3/7 < p \leqslant p_W \approx 0.696$, and to the GHZ\W class for $p > p_W$ [51,52]. The plot in Fig. 4 shows that the class transition in p_B occurs between $p = 0.43$ and $p = 0.44$, which is only slightly higher than p_B, which is expected since the algorithm gives a close lower bound to the optimal value. In addition, the numerical values in the graph show the transition between classes W\B and GHZ\W.

V. CONCLUSION

We explored the theory of LSIP to derive properties of the dual problem of the convex roof procedure that gives entanglement monotones for mixed states from pure state measures. We showed that the absence of the duality gap between primal and dual problems occurs in very general conditions. In addition, we proved that the set of optimal points is nonempty and bounded and we derived bounds on the coefficients of optimal solutions. For numerical calculations, we wrote the dual problem in a suitable LSIP form and adapted a CCPA designed for this type of optimization. To check the performance of the algorithm, we calculated two measures of genuine three-qubit entanglement, three-tangle and π-tangle, for the mixture of GHZ and W states and for the generalized Werner states, a full rank family of states. We compared the numerical results with the available analytical values and verified that the CCPA results are very close the exact ones for the lower rank family of states, while providing lower bounds for the high-rank ones. As the algorithm gives lower bounds on the amount of entanglement for suboptimal feasible points and global convergence, the results are in agreement with the expected

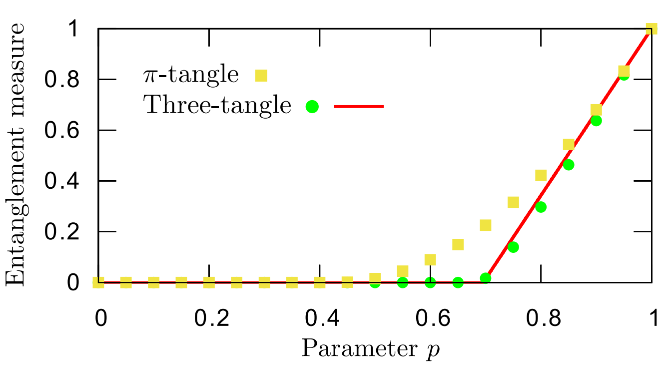

FIG. 2. Three-tangle and π-tangle calculated for states ρ'_p. Symbols (boxes and circles) and the continuous line represent numerical and analytical values, respectively.

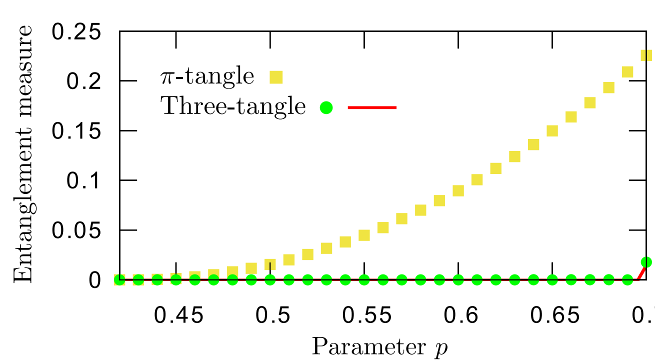

FIG. 4. Three-tangle and π-tangle calculated for states ρ'_p. Symbols (boxes and circles) and the continuous line represent numerical and analytical values, respectively.

behavior. Furthermore, we used the difference between the two measures to distinguish GHZ\W and W classes, in agreement with the entanglement classification of these states in the literature.

We believe that our work gives a good alternative to the convex roof calculation of mixed-state entanglement, especially when close lower bounds are required. The CCPA has very general applicability, working with discontinuous measures and multipartite states with any finite rank. For future works, we expect to apply other LSIP algorithms to the convex roof problem, with the necessary modifications and improvements.

ACKNOWLEDGMENTS

The authors acknowledge the financial support of the Brazilian agencies CNPq (Grants No. 312723/2018-0, No. 306065/2019-3, and No. 425718/2018-2), CAPES (PROCAD - 2013), FAPEG (PRONEM Grant No. 201710267000540, PRONEX Grant No. 201710267000503), and CAPES/FAPEG (Grant DOCFIX No. 201810267001518) for the fellowship of T. M. Carrijo. This work was also performed as part of the Brazilian National Institute of Science and Technology (INCT) for Quantum Information (Grant No. 465469/2014-0).

APPENDIX A: THEORETICAL PROPERTIES OF PROBLEMS *P* AND D_ρ

In this section, we prove the three theoretical properties of problems P and D_ρ listed in Sec. III A.

Proof of properties 1, 2 and 3. The first-moment cone of the linear semi-infinite system σ_ρ is given by $M_c \equiv \text{cone}(\mathcal{E}_\rho)$ [44], which is the set of all conical combinations of elements of $\mathcal{E}_\rho$. As cone($\mathcal{E}_\rho$) is the cone of positive semidefinite matrices of H_ρ, we have that $\text{int}(M_c) \neq \emptyset$. As ρ is a full rank matrix of H_ρ, then $\rho \in \text{int}(M_c)$. By Theorem 8.1 of Ref. [44], we conclude that there exists an optimal solution X^*_ρ of D_ρ and that the set of all optimal solutions F^*_ρ is bounded. Furthermore, by the same theorem, we could conclude the absence of the duality gap without making the continuity hypothesis on E. ■

APPENDIX B: THREE-TANGLE AND π-TANGLE FOR FAMILIES OF STATES

Here, we show the analytical expressions for the three-tangle and π-tangle for the families of states ρ_p and ρ'_p available in the literature. First, we show the formulas for the three-tangle quantifier applied to the mixture of GHZ and W states: ρ_p. Setting $s \equiv 8\sqrt{6}/9$, $p_0 \equiv s^{2/3}/(1+s^{2/3})$, and $p_1 \equiv 1/2 + 1/(2\sqrt{1+s^2})$, the three-tangle of ρ_p is given by [12,13]

$$\tau(\rho_p) = \begin{cases} 0 & \text{for } p \leqslant p_0, \\ \tau_3(p,0) & \text{for } p_0 < p \leqslant p_1, \\ \tau_3^{\text{conv}}(p,p_1) & \text{for } p > p_1, \end{cases} \tag{B1}$$

where $\tau_3(p,0) \equiv |p^2 - 16\sqrt{p(1-p)^3}/3\sqrt{6}|$ and $\tau_3^{\text{conv}}(p,p_1) \equiv [p - p_1 + (1-p)(p_1^2 - s\sqrt{p_1(1-p_1)^3})]/(1-p_1)$.

The family of states ρ'_p, as the parameter p ranges from 0 to 1, goes through all three-qubit entanglement classes: S, B\S, W\B, and GHZ\W [52], where S and B are the classes of separable and biseparable states, respectively. The value p_W of p that separates the classes W and GHZ\W is $p_W \approx 0.6955427$. The three-tangle of ρ'_p is then given by [36]

$$\tau(\rho'_p) = \begin{cases} 0 & \text{for } p \leqslant p_W, \\ \frac{p-p_W}{1-p_W} & \text{for } p_W < p \leqslant 1. \end{cases} \tag{B2}$$

The last available analytical result is the π-tangle of the states ρ_p, which is given by [41]

$$\pi(\rho_p) = \begin{cases} \pi^{(1)}(\rho_p) & \text{for } 0 \leqslant p \leqslant p_0, \\ \pi^{(2)}(\rho_p) & \text{for } p_0 < p \leqslant p_1, \\ \pi^{(3)}(\rho_p) & \text{for } p_1 < p \leqslant 1, \end{cases} \tag{B3}$$

where $\pi^{(1)}(\rho_p) \equiv \{4(\sqrt{5}-1)(p_0 - p) + p[5p_0^2 - 4p_0 + 8 - 18(\sum_{i=1}^4 |\lambda_i(p_0)| - 1)^2]\}/9p_0$, $\pi^{(2)}(\rho_p) \equiv [5p^2 - 4p + 8 - 18(\sum_{i=1}^4 |\lambda_i(p)| - 1)^2]/9$, and $\pi^{(3)}(\rho_p) \equiv \{p - p_1 + (1-p)[5p_1^2 - 4p_1 + 8 - 18(\sum_{i=1}^4 |\lambda_i(p_1)| - 1)^2]/9\}/(1-p_1)$. For a fixed value of p, each $\lambda_i(p)$, for $i \in \{1,\dots,4\}$, is a solution of the following equation:

$$\lambda^4 - \lambda^3 + \left(\frac{5}{36}p^2 - \frac{p}{9} + \frac{2}{9}\right)\lambda^2 + \left[\frac{[p(1-p)]^{3/2}}{3\sqrt{6}} - \frac{7}{27}p^3 + \frac{7}{18}p^2 - \frac{p}{6} + \frac{1}{27}\right]\lambda + \left[-\frac{p[p(1-p)]^{3/2}}{6\sqrt{6}} - \frac{41}{648}p^4 + \frac{149}{648}p^3 - \frac{13}{54}p^2 + \frac{7}{81}p - \frac{1}{81}\right] = 0.$$

APPENDIX C: BOUNDING THE FEASIBLE SET

The proof of Corollary 1, stated in Sec. III B, is given after Lemma 1.

Lemma 1. If $0 \leqslant E([\psi]) \leqslant 1, \forall[\psi] \in \mathcal{E}_\rho$, and $\delta \equiv (r-1)\lambda_r/\lambda_1$, where $r = \text{rank}(\rho)$, λ_1 and λ_r are the lowest and highest eigenvalues of ρ, respectively, then $F^*_\rho \subseteq B_\delta$.

Proof. Let $x_1 \leqslant \dots \leqslant x_r$ be the eigenvalues of $X \in H_\rho$. By the constraint $E([\psi]) + \text{Tr}([\psi]X) \geqslant 0, \forall[\psi] \in \mathcal{E}_\rho$, of the problem D_ρ and the min-max theorem, we have that $x_1 \geqslant -1$ is a necessary condition for the feasibility of X. Let $\{|x_1\rangle, \dots |x_r\rangle\}$ be an orthonormal basis with eigenvectors of X and $\rho = \sum_{k,l} \lambda'_{k,l}|x_k\rangle\langle x_l|$. As $x_1 \geqslant -1$, $0 \leqslant E^\cup(\rho) \leqslant 1$, and by the fact that there is no duality gap between D_ρ and P, if $X \in F^*_\rho$ then

$$\text{Tr}(\rho X) = \sum_k \lambda'_{k,k}x_k \leqslant 0 \Rightarrow x_r \leqslant (r-1)\frac{\lambda_r}{\lambda_1}. \tag{C1}$$

Equation (C1) implies that $\|X\| = \sup\{\|X|\psi\rangle\|_2 : \||\psi\rangle\|_2 = 1\} = \max\{|x_1|, |x_r|\} \leqslant (r-1)\lambda_r/\lambda_1$. Thus, we conclude that $F^*_\rho \subseteq B_\delta$ for $\delta \equiv (r-1)\lambda_r/\lambda_1$. ■

Now, the proof of Corollary 1:

Proof. Let $\{|x_1\rangle, \dots |x_r\rangle\}$ be an orthonormal basis with eigenvectors of X and $X = \sum_k x_k[x_k]$. By Lemma 1, $|\text{Tr}(Z_m X)| \leqslant \sum_k |x_k||\text{Tr}(Z_m[x_k])| \leqslant \sum_k |x_k| \leqslant r(r-1)\lambda_r/\lambda_1$. ■

APPENDIX D: THE PSEUDOCODE OF THE CENTRAL CUTTING-PLANE ALGORITHM (CCPA)

The original pseudocode of the CCPA is found in Ref. [49]. Our description of it, step by step, with the necessary modifications, including the addition of a tolerance $\epsilon > 0$, and without the deletion rules is given below.

Step 0: Let $\bar{E}$ be strictly greater than $-v(D_c)$. Let SD_c^0 be the program

$$\max_{(y,x)\in\mathbb{R}^{r^2+1}} \quad y,$$

$$\text{subject to} \quad \langle c, x\rangle + y\|c\|_2 \leqslant \bar{E},$$

$$|x_m| \leqslant r(r-1)\frac{\lambda_r}{\lambda_1},\ 1 \leqslant m \leqslant r^2. \tag{D1}$$

Choose $w^{(0)} \in \mathbb{R}^{r^2}$ such that $|w^{(0)}| \leqslant r(r-1)\lambda_r/\lambda_1$, $1 \leqslant m \leqslant r^2$. Let $k = 1$.

Step 1: Let $(x^{(k)}, y^{(k)}) \in \mathbb{R}^{r^2+1}$ be a solution of SD_c^{k-1}. If $|y| < \epsilon$, stop. Otherwise, go to step 2.

Step 2: (i) If $v(D_{\text{aux}}^k) \geqslant 0$, where $D_{\text{aux}}^k : \inf_{\psi\in\tilde{\mathcal{E}}_c} \tilde{E}(\psi) + \langle\psi, x^{(k)}\rangle$, add the constraint $\langle c, x\rangle + y\|c\|_2 \leqslant \langle c, x^{(k)}\rangle$ to program SD_c^{k-1}. Set $w^{(k)} = x^{(k)}$.

(ii) Otherwise, add the constraint $\langle\psi^{(k)}, x\rangle - y\|\psi^{(k)}\|_2 \geqslant -\tilde{E}(\psi^{(k)})$ to program SD_c^{k-1}. Set $w^{(k)} = w^{(k-1)}$.

In either case, call the resulting program SD_c^k. Set $k = k + 1$ and return to step 1.

[1] A. Einstein, B. Podolsky, and N. Rosen, Phys. Rev. **47**, 777 (1935).
[2] J. S. Bell, Physics **1**, 195 (1964).
[3] B. Hensen, H. Bernien, A. E. Dréau, A. Reiserer, N. Kalb, M. S. Blok, J. Ruitenberg, R. F. L. Vermeulen, R. N. Schouten, C. Abellán, W. Amaya, V. Pruneri, M. W. Mitchell, M. Markham, D. J. Twitchen, D. Elkouss, S. Wehner, T. H. Taminiau, and R. Hanson, Nature (London) **526**, 682 (2015).
[4] N. Lambert, C. Emary, and T. Brandes, Phys. Rev. Lett. **92**, 073602 (2004).
[5] K. C. Tan, S. Choi, H. Kwon, and H. Jeong, Phys. Rev. A **97**, 052304 (2018).
[6] V. Vedral, New J. Phys. **6**, 102 (2004).
[7] L. Prochaska, X. Li, D. C. MacFarland, A. M. Andrews, M. Bonta, E. F. Bianco, S. Yazdi, W. Schrenk, H. Detz, A. Limbeck, Q. Si, E. Ringe, G. Strasser, J. Kono, and S. Paschen, Science **367**, 285 (2020).
[8] R. Horodecki, P. Horodecki, M. Horodecki, and K. Horodecki, Rev. Mod. Phys. **81**, 865 (2009).
[9] L. Gyongyosi and S. Imre, Comp. Sci. Rev. **31**, 51 (2019).
[10] L. Pezzè, A. Smerzi, M. K. Oberthaler, R. Schmied, and P. Treutlein, Rev. Mod. Phys. **90**, 035005 (2018).
[11] G. Vidal, J. Mod. Opt. **47**, 355 (2000).
[12] R. Lohmayer, A. Osterloh, J. Siewert, and A. Uhlmann, Phys. Rev. Lett. **97**, 260502 (2006).
[13] C. Eltschka, A. Osterloh, J. Siewert, and A. Uhlmann, New J. Phys. **10**, 043014 (2008).
[14] K. Życzkowski, Phys. Rev. A **60**, 3496 (1999).
[15] K. Audenaert, F. Verstraete, and B. De Moor, Phys. Rev. A **64**, 052304 (2001).
[16] B. Röthlisberger, J. Lehmann, and D. Loss, Phys. Rev. A **80**, 042301 (2009).
[17] K. Cao, Z.-W. Zhou, G.-C. Guo, and L. He, Phys. Rev. A **81**, 034302 (2010).
[18] B. Röthlisberger, J. Lehmann, and D. Loss, Comput. Phys. Commun. **183**, 155 (2012).
[19] S. Ryu, S.-S. B. Lee, and H.-S. Sim, Phys. Rev. A **86**, 042324 (2012).
[20] G. Tóth, T. Moroder, and O. Gühne, Phys. Rev. Lett. **114**, 160501 (2015).
[21] F. G. S. L. Brandão, Phys. Rev. A **72**, 022310 (2005).
[22] I. Bengtsson and K. Zyczkowski, *Geometry of Quantum States*, 2nd ed. (Cambridge University Press, Cambridge, UK, 2006), Chap. 17, pp. 493–543.
[23] D. Bruß and C. Macchiavello, Phys. Rev. A **83**, 052313 (2011).
[24] M. Pan, D. Qiu, and S. Zheng, Quant. Info. Proc. **16**, 211 (2017).
[25] A. Cabello, arXiv:quant-ph/0009025.
[26] M. Epping, H. Kampermann, C. Macchiavello, and D. Bruß, New J. Phys. **19**, 093012 (2017).
[27] G. Murta, F. Grasselli, H. Kampermann, and D. Bruß, arXiv:2003.10186.
[28] D. M. Greenberger, M. A. Horne, A. Shimony, and A. Zeilinger, Am. J. Phys. **58**, 1131 (1990).
[29] P. Hauke, M. Heyl, L. Tagliacozzo, and P. Zoller, Nat. Phys. **12**, 778 (2016).
[30] J. Smith, A. Lee, P. Richerme, B. Neyenhuis, P. W. Hess, P. Hauke, M. Heyl, D. A. Huse, and C. Monroe, Nat. Phys. **12**, 907 (2016).
[31] V. Coffman, J. Kundu, and W. K. Wootters, Phys. Rev. A **61**, 052306 (2000).
[32] A. Miyake, Int. J. Quantum. Inform. **02**, 65 (2004).
[33] Y.-C. Ou and H. Fan, Phys. Rev. A **75**, 062308 (2007).
[34] Y. Guo and L. Zhang, Phys. Rev. A **101**, 032301 (2020).
[35] S. Hill and W. K. Wootters, Phys. Rev. Lett. **78**, 5022 (1997).
[36] J. Siewert and C. Eltschka, Phys. Rev. Lett. **108**, 230502 (2012).
[37] A. Acín, D. Bruß, M. Lewenstein, and A. Sanpera, Phys. Rev. Lett. **87**, 040401 (2001).
[38] W. Dür, G. Vidal, and J. I. Cirac, Phys. Rev. A **62**, 062314 (2000).
[39] G. Vidal and R. F. Werner, Phys. Rev. A **65**, 032314 (2002).
[40] V. Vedral, M. B. Plenio, M. A. Rippin, and P. L. Knight, Phys. Rev. Lett. **78**, 2275 (1997).
[41] T. Ma and S.-M. Fei, in *Quantum Bio-Informatics V: Proceedings of Quantum Bio-Informatics 2011*, Vol. 30, edited by L. Accardi, W. Freudenberg, and M. Ohya (World Scientific, Singapore, 2013), pp. 425–434.
[42] J. Eisert, F. G. S. L. Brandão, and K. M. R. Audenaert, New J. Phys. **9**, 46 (2007).
[43] R. Reemtsen and J.-J. Rückmann (eds.), *Semi-infinite Programming*, 1st ed., Nonconvex Optimization and Its Applications Vol. 25 (Springer, Boston, MA, 1998).
[44] M. A. Goberna and M. A. López, *Linear Semi-infinite Optimization*, edited by B. Brosowski and G. F. Roach (John Wiley & Sons, New York, 1998).
[45] S.-S. B. Lee and H.-S. Sim, Phys. Rev. A **85**, 022325 (2012).
[46] M. Horodecki, P. Horodecki, and R. Horodecki, Phys. Lett. A **283**, 1 (2001).

[47] B. M. Terhal, Theor. Comput. Sci. **287**, 313 (2002).
[48] M. A. Goberna and M. A. López, 4OR-Q. J. Oper. Res. **15**, 221 (2017).
[49] P. R. Gribik, in *Semi-infinite Program*, edited by R. Hettich (Springer-Verlag, Berlin, 1979), pp. 66–82.
[50] B. Betrò, Math. Program. **101**, 479 (2004).
[51] O. Gühne and M. Seevinck, New J. Phys. **12**, 053002 (2010).
[52] C. Eltschka and J. Siewert, Phys. Rev. Lett. **108**, 020502 (2012).